ACS OMEGA

Open Access

http://pubs.acs.org/journal/acsodf

Article

Thermal-Responsive Smart Windows with Passive Dimming and Thermal Energy Storage

Haiquan Zhang,*,† Ling Wang,† Fuge Wang,† Qiaoming Fang, Songjiao Chen, Wei He, and Ning Wang*

Cite This: *ACS Omega* 2024, 9, 27222−27231

Read Online

ACCESS | Metrics & More | Article Recommendations | Supporting Information

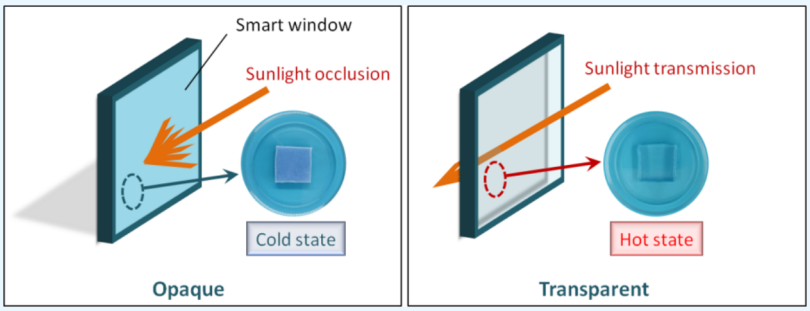

ABSTRACT: Chromogenic smart windows are one of the key components in improving the building energy efficiency. By simulation of the three-dimensional network of polymer hydrogels, thermal-responsive phase change materials (TRPCMs) are manufactured for energy-saving windows. For simulated polymer hydrogels, tetradecanol (TD) and a color changing dye (CCD) are filled in situ in poly(*n*-butyl isobutyrate) (PBB) networks. TRPCMs convert solar energy into thermal energy through a dark blue CCD. The TD phase change material (PCM) absorbs heat energy to become a transparent liquid. Simultaneously, the CCD changes from blue to colorless and transparent at around 45 °C. As a result, as-prepared TRPCMs transform from an opaque state at room temperature to a high-transparency state after melting (74.5%). TRPCMs also show a good thermal storage capacity, with a phase transition enthalpy exceeding 161.9 J g^{-1}. As-prepared smart materials can simultaneously achieve photothermal conversion, thermal energy diffusion, latent heat storage, and resistance to liquid leakage at the phase interface between opaque and transparent states, providing more options for the design of energy-saving buildings.

1. INTRODUCTION

Heating, ventilation, and air-conditioning (HVAC) systems account for approximately 40−60% of the energy usage in buildings or 15% of the world's total energy consumption.[1−3] Statistical surveys show that increasing the cooling temperature by 1 °C can reduce the building energy consumption by 10−25%.[4,5] Generally, glass windows are considered the least energy-efficient part of the building envelope structure. 82% transmittance means that most of the sunlight can enter the room through the glass window, increasing the cooling load.[6,7] About one-third of the building energy consumption is wasted on windows due to the high thermal conductivity of inorganic glass reaching 1.1 W m^{-1} K^{-1}.[8,9] To address this issue, improving the window energy efficiency is crucial for energy conservation.

Energy-saving windows focus on breakthroughs in color rendering technology, including electrochromic,[10,11] photochromic,[12,13] thermochromic,[14,15] and pressure-induced color.[16,17] Examples of chromogenic materials include hydrogel,[18,19] vanadium dioxide,[20,21] and organic glass loaded with the phase change material (PCM).[22,23] Thermoresponsive smart windows equipped with poly(*N*-isopropylacrylamide) (PNIPAm) aqueous solution could cut off 44.6% HVAC energy consumption compared with normal glass.[24] Mandal et al. reported porous polymer coatings with switchable optical transmittance.[25] However, it is an inevitable challenge to further improve the energy-saving capability of the chromogenic windows due to the lack of energy storage mechanisms.

Solid−liquid PCMs store thermal energy at almost constant temperatures while undergoing a reversible transition from an opaque crystalline material to a transparent liquid. Therefore, solid−liquid PCMs have the dual advantages of energy storage and dimming, making them one of the most promising candidate materials for energy-saving glass.[26,27] Polymers are usually used to encapsulate solid−liquid materials to prevent liquid leakage from the PCM.[28,29] Note that polymers must have compatibility and a well-matched refractive index with phase change materials. Otherwise, composite phase change

Received: February 18, 2024
Revised: May 29, 2024
Accepted: June 5, 2024
Published: June 13, 2024

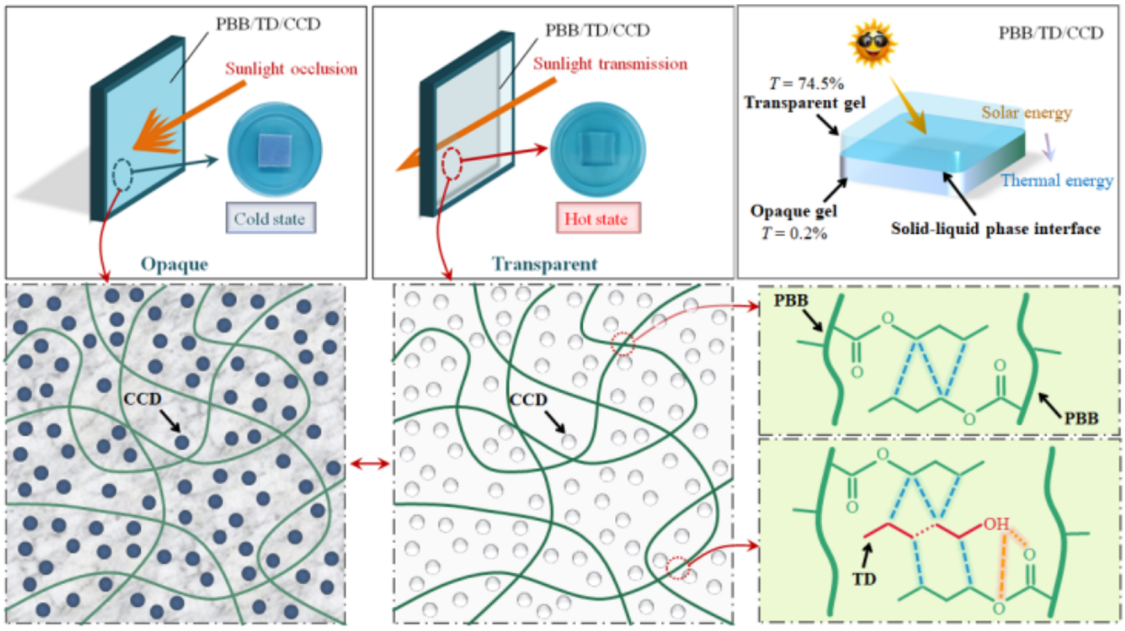

Figure 1. Design strategy for the thermally responsive PBB/TD/CCI functional material.

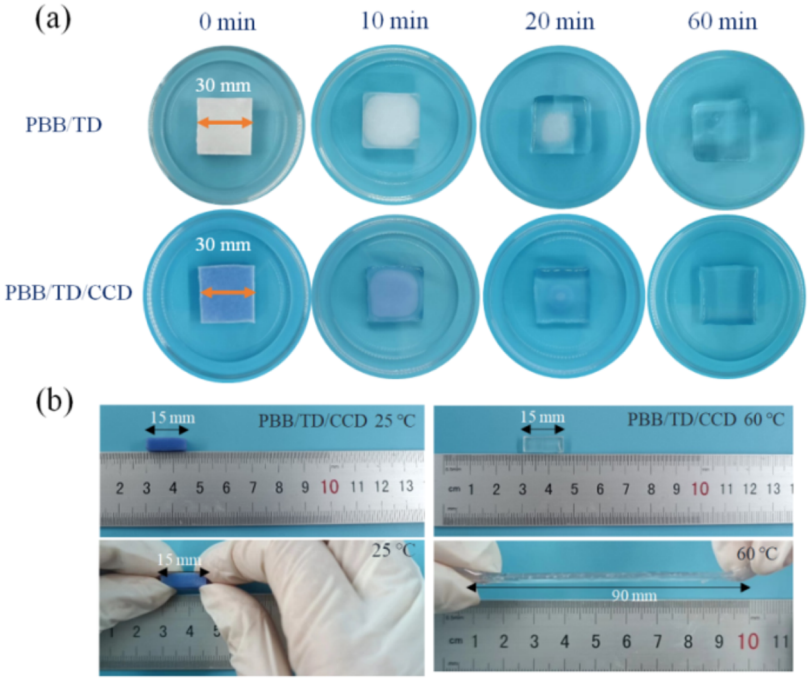

Figure 2. Characterization of the liquid leakage resistance of the PBB/TD/CCI-2 composite at 60 °C. (a) Heating experiments. (b) Stretchable experiments.

materials no longer have a switchable optical transmittance. For example, Zhang et al. dispersed the polyethylene glycol PCM in the polyacrylamide hydrogel, but the resulting composite was still white even in a high-temperature environment.[30]

Herein, thermal-responsive poly(*n*-butyl isobutyrate) (PBB)/tetradecanol (TD)/color changing dye (CCD) PCMs were designed by introducing the tetradecanol PCM and a commercial color changing dye into the poly(*n*-butyl isobutyrate) networks. PBB and TD, respectively, simulated the three-dimensional framework and non flowing water of the polymer hydrogel, and the CCD played the role of a photothermal conversion medium. Thermal-responsive PBB/TD/CCD materials achieved photothermal conversion, heat diffusion, and latent heat storage within the same microzone, with the microzone changing from a blue opaque state (T_{trans}, 0.2%) to a transparent state (T_{trans}, 74.5%). Therefore, as-prepared PBB/TD/CCD thermal-responsive PCMs (TRPCMs) can be applied in smart windows in high-latitude energy-saving buildings.

2. RESULTS AND DISCUSSION

2.1. Preparation of the Thermal-Responsive Organic Glass. The preparation was a rather simple process of mixing

https://doi.org/10.1021/acsomega.4c01570
ACS Omega 2024, 9, 27222−27231

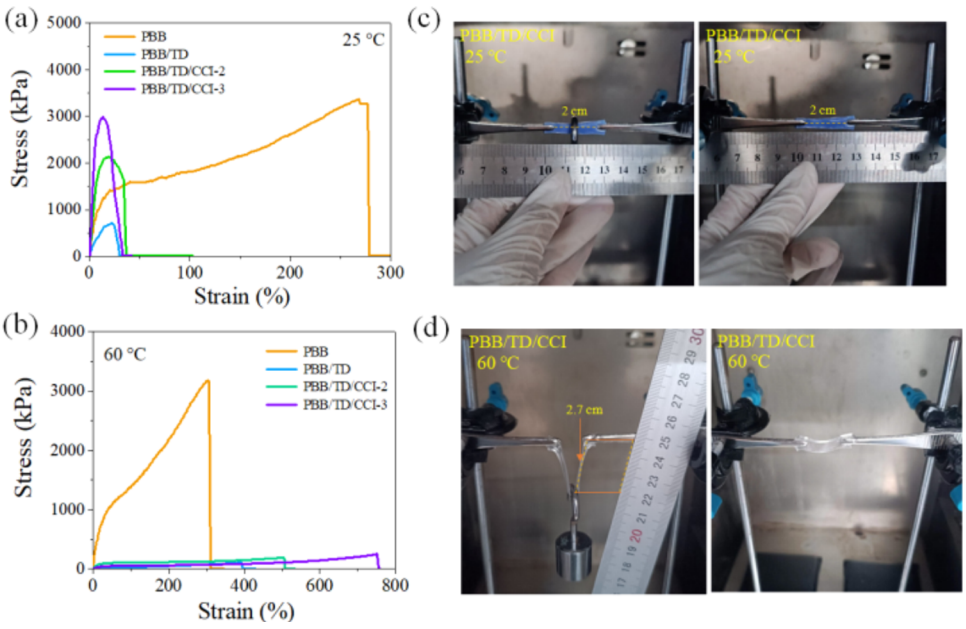

Figure 3. Stretchability experiments of the PBB, PBB/TD, and PBB/TD/CCD samples. (a) Stress−strain curves of the PBB and PBB/TD composites at 25 °C. (b) Stress−strain curves at 60 °C. (c) Digital photographs of the PBB/TD/CCD-2 composite at 25 °C. (d) Digital photos at 60 °C.

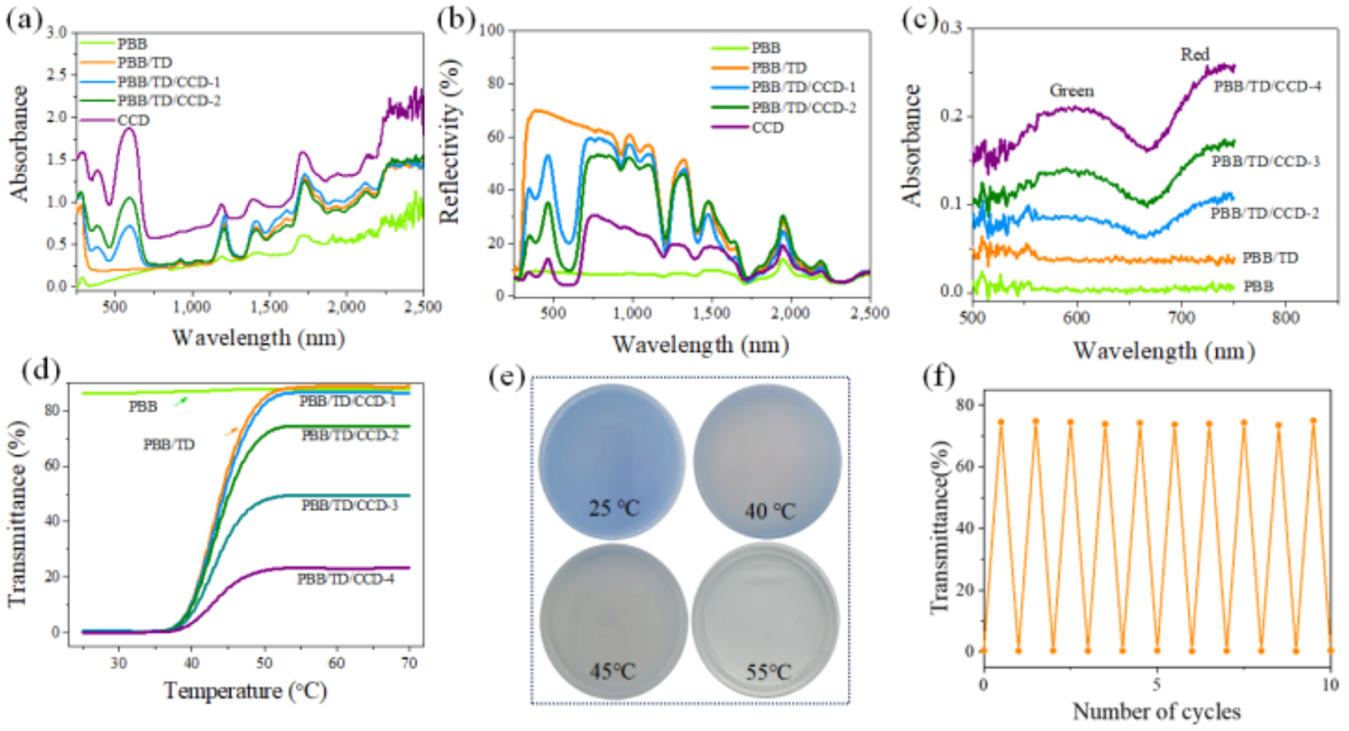

Figure 4. Optical properties of thermally responsive PBB/TD/CCD materials. (a) Visible absorption spectrum at 25 °C. (b) Reflectivity spectrum at 25 °C. (c) Visible absorption spectrum at 42 °C. (d) Transmittance−temperature curves. (e) Digital photos of the PBB/TD/CCD-2 at different temperatures. (f) Transmittance cycle curve of the PBB/TD/CCD-2.

n-butyl methacrylate, the TD PCM, and the CCD with an AIBN chain initiator and an EGDMA cross-linking agent, followed by thermal-induced polymerization of the BB monomer at 65 °C for 24 h.[31] The reversible temperature-sensitive CCD is prepared from an electron transfer organic compound system. Electron transfer organic compounds are a class of organic chromophores with special chemical structures. At a specific temperature, the molecular structure of the organic compound undergoes a change due to electron transfer, resulting in a color change. This color changing substance not only has bright colors but can also achieve color changes from "colored−colorless" to "colorless−colored" states (Figure S1).

The design of thermal-responsive PBB/TD/CCD PCMs is based on three objectives, as shown in Figure 1: (1) The PBB polymer with the color changing dye changes from a blue color

https://doi.org/10.1021/acsomega.4c01570
ACS Omega 2024, 9, 27222−27231

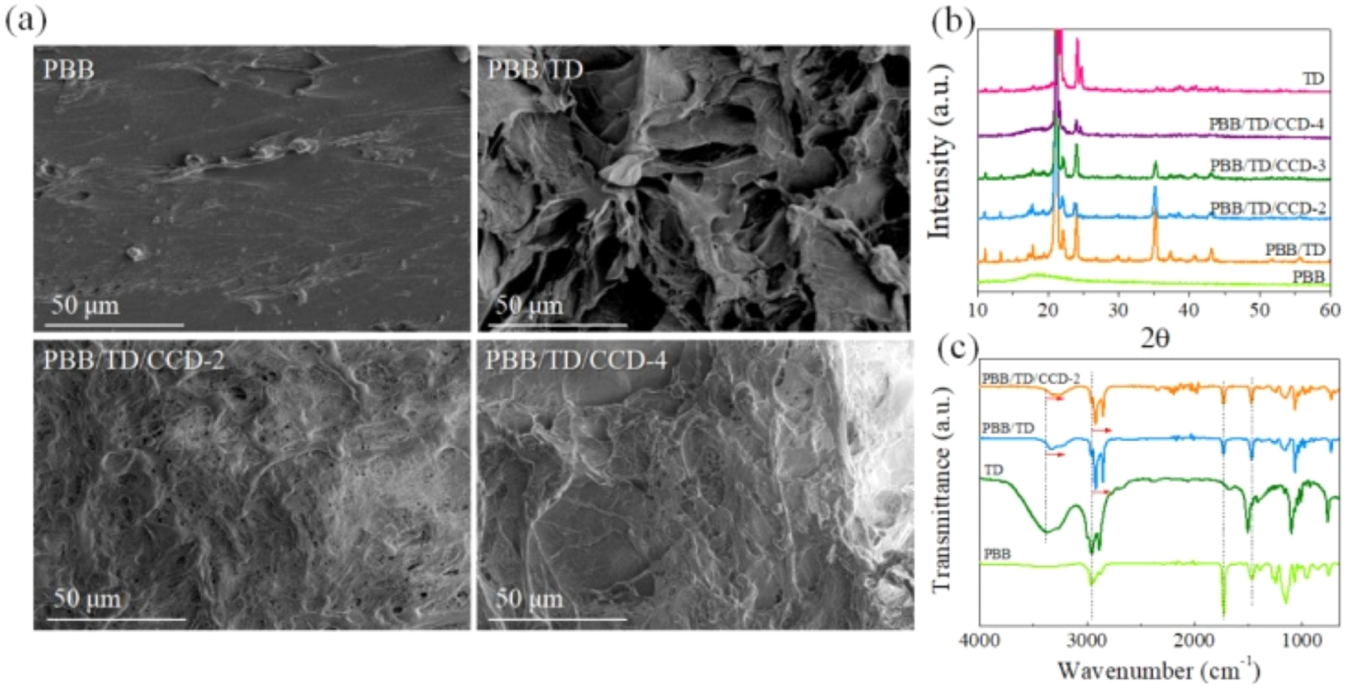

Figure 5. Physical performance characterization. (a) FE-SEM images of the pure PBB, PBB/TD, and PBB/TD/CCD composites. (b) XRD patterns. (c) FT-IR patterns.

at room temperature (improving the photothermal conversion efficiency) to a transparent state (increasing transparency), as shown in Figure S2. (2) The white TD PCM absorbs heat from CCD microparticles and converts it into a transparent liquid. (3) The well-matched refractive index between the TD liquid and PBB (n_{TD}/n_{PBB} = 1.43:1.42) results in a high transmittance of 74.5% for the PBB/TD/CCD at 55 °C. That is to say, photothermal conversion, heat transfer, and latent heat storage have been achieved at the interface microregion between transparent and opaque states. This design eliminates the spatial location difference between solar energy conversion and thermal energy storage, no longer requiring an increase in the material's thermal conductivity.

2.2. Characterization of the Physical Properties of the PBB/TD/CCI Composite. As shown in Figure 2, digital photos demonstrate the antiliquid leakage of the PBB/TD/CCD PCM. For the PBB/TD/CCD-2 with a V_{PBMA}/V_{MA} volume ratio of 2:3, it is impossible to observe the melted TD liquid phase with the naked eye, as shown in Figure 2a. Even when stretched to 600% of the initial length at 60 °C, the PBB/TD/CCD-2 TRPCM did not observe any liquid overflow, as shown in Figure 2b. Note that the PBB/TD/CCD composite exhibits switchable characteristics of stretchability, color, and transmittance at high-low temperatures.

Stretching experiments were carried out for as-prepared PBB, PBB/CCD, and PBB/TD/CCD samples of 2 mm thickness, 4 mm width, and 20 mm gauge length at a loading rate of 100 mm min^{-1}. As shown in Figure 3, the pure PBB polymer presents a fracture strain of 274% and a fracture stress of 3300 kPa, and its mechanical properties are independent of the temperature. When the TD PCM is introduced into the PBB three-dimensional network, the fracture stress/strain of the PBB/CCD and PBB/TD/CCD composites is significantly reduced, as shown in Figure 3a. However, highly dispersed color changing dyes can enhance the fracture strength of composite materials. For example, the fracture strain of PBB/TD/CCD-3 increased from 690 kPa of PBB/TD to 2980 kPa, but the fracture strain of both the composites was 33%. As-prepared PBB/CCD and PBB/TD/CCD PCMs transform into a good flexible material at 60 °C. Thermal-responsive phase change materials can self-recover to its original shape within a few minutes of release of the stress. The PBB/TD/CCD-3 designed in imitation of the polymer hydrogel exhibits a superelastic characteristic (fracture strain, 750%) at 60 °C, because the molten TD phase liquid reduces the cross-linking of the poly *n*-butyl isobutyrate three-dimensional network. The tangential stretching experiments shown in Figure 3c,d further prove the switchable stretchability and self-recovery performances.

To demonstrate its switchable optical transmittance, the visible light absorption, reflectivity, and transmittance spectra of the PBB/TD/CCD PCM were characterized at 25 °C.[32−34] Within the visible light wavelength range 380−750 nm, neither the PBB organic glass nor the PBB/TD PCM composite exhibited any absorption peaks (Figure 4a). This is due to the high transmittance of PBB (~90%, Figure S3) and the high reflectivity of PBB/TD (60−70%, Figure 4b). The PBB/TD/CCD samples exhibit absorption of red light in the visible light band and also exhibit good absorption characteristics in infrared fluctuations. That is, CCD indeed improves the absorption efficiency of the composite for sunlight.

According to Figure 4c, neither the PBB packaging medium nor the TD PCM liquid exhibits absorption bands at 42 ± 2 °C in the wavelength range of 540−750 nm. However, the as-prepared PBB/TD/CCD FSPCM exhibits two distinct absorption bands within the same wavelength, and the absorption intensity is positively correlated with the content of the color changing dye. When PBB/TD/CCD-2 is heated to 60 °C, the corresponding green and red absorption bands disappear, as shown in Figure S4.

The transmittance curves of the PBB, PBB/TD, and PBB/TD/CCD samples at 25−70 °C were characterized online by

https://doi.org/10.1021/acsomega.4c01570
ACS Omega 2024, 9, 27222−27231

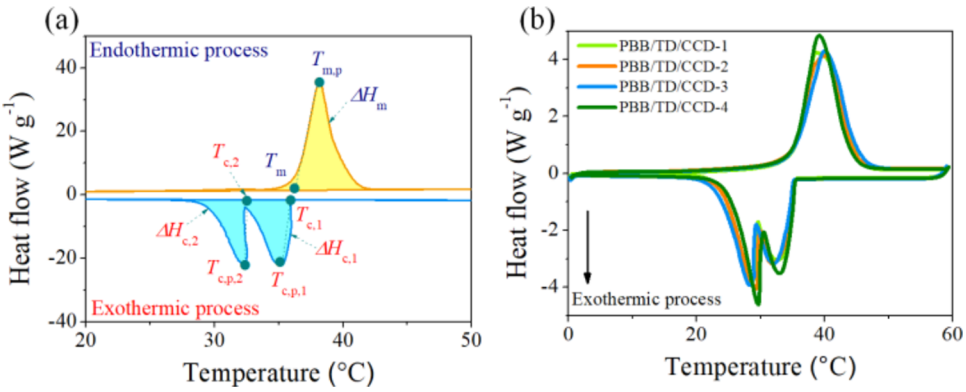

Figure 6. Heat absorption/release curves of PCM composite materials. (a) DSC curve of the pure TD PCM. (b) DSC curves of the PBB/TD/CCD composites.

the LS116 transmittance tester with the full wavelength range of visible light (380−760 nm). According to Figure 4d, the pure PBB polymer exhibits a high transmittance (about 87.0%) independent of the temperature due to the amorphous nature of polymer molecular chains. The PBB/TD and PBB/TD/CCD composites with a thickness of 1.0 mm exhibit a good switchable optical transparency at 35−55 °C, based on the melting/solidification of the TD PCM encapsulated in the PBB medium. The visualization result shows that the PBB/TD/CCD-2 sample transitions from a blue color at 35 °C to a transparent state at 60 °C, as shown in Figure 4c. Note that the transmittance decreases from 88.3% of the PBB/TD to 23.3% of the PBB/TD/CCD-4 at 55 °C due to the refraction or scattering of visible light by CCD micro/nanoparticles. We chose the PBB/TD/CCD-2 composite as the smart glass because its transmittance (74.5%) is similar to that of ordinary glass. Figure 4d shows the transmittance cycle curve of the PBB/TD/CCD-2 composite at 25 and 55 °C, indicating the stability of switchable transmittance.

To understand the switchable optical transparency of the PBB/TD/CCD samples, field emission scanning electron microscopy (FE-SEM), X-ray diffraction (XRD), and infrared (IR) absorption spectrometry were characterized, and the corresponding test results are displayed in Figure 5. The pure PBB polymer exhibits a dense microscopic morphology on the cross-section (Figure 5a) based on the cross-linking of molecular chains. Note that the interaction between molecular chains does not lead to polymer crystallization (Figure 5b); therefore, the pure PBB polymer exhibits ultrahigh transmittance. The amorphous nature of polymers was also observed in poly(methyl methacrylate) (Figure S5, Supporting Information). When the TD PCM is introduced into the PBB polymer network, the PBB/TD composite tends to have an irregular porous morphology, as shown in Figure 5a. A large number of dispersed microparticles were observed at the cross-section of PBB/TD/CCD composites, which belong to the color changing dye. Interestingly, the color changing dye particles restore the dense form for the PBB/TD/CCD composites. All characteristic diffraction peaks of the PBB/TD/CCD composites originate from the TD PCM, as shown in Figure 5b. Therefore, there is no chemical reaction between the PBB polymer network, the TD PCM, and the CCD photothermal conversion medium. The pure TD PCM exhibits two infrared absorption peaks at 3380 and 1495 cm^{-1}, attributed to the terminal hydroxyl group.[35] For the PBB/TD composite, the vibration absorption peak (left) of −OH shifts to 3325 cm^{-1}, and the intensity of the absorption peak decreases significantly. The infrared absorption peak (right) of −OH coincides with the vibrational absorption peak of the ester group in the PBB polymer network. The FT-IR results indicate that TD and PBB exhibit cross-linking (hydrogen bond). For the pure PBB and TD samples, two stretching vibrational absorption peaks attributed to −CH are observed at 2942 and 2880 cm^{-1}.[36] When PBB and TD are physically mixed, the corresponding vibrational peaks of −CH shift to the right to 2915 and 2852 cm^{-1}, respectively. This indicates that the carbon chain of TD has also undergone cross-linking with the side chain of PBB. The introduction of the color changing dye does not increase the number of characteristic absorption peaks of PBB/TD, nor do these peaks show a significant shift. This indicates that the CCD cannot undergo chemical cross-linking with PBB or TD.

2.3. Characterization of the Thermal Storage Performance. Figure 6 exhibits the thermal storage performances of the TD, PBB/TD, and PBB/TD/CCD PCMs. Measurement methods for the phase transition temperature (T) and energy storage density (ΔH) of materials are summarized in Figure 6a.[37,38] The pure TD PCM displays one endothermic peak at 35−42 °C and two exothermic peaks at 28−36 °C. The corresponding energy storage density is as high as 237.4 J g^{-1}. After encapsulating the TD PCM with a PBB polymer network, the energy storage density of PBB/TD/CCD composites decreases to 161.9−173.7 J g^{-1} (Figure 6b). Note that the PBB packaging medium widens the endothermic (27−49 °C) and exothermic (20−37 °C) peaks of the TD PCM. Figure S6 shows the temperature−time curves of the PCM materials in a constant temperature chamber. The pure PBB polymer participates in the storage/release of heat through sensible heat, but the first isothermal exothermic platform of the pure TD PCM is located at 37.3 °C. After encapsulation with the PBB polymer network, the isothermal exothermic plateau of the PBB/TD composite decreases by 2.3 °C, as shown in Figure S7. The self-dispersed CCD particles further reduce the exothermic platform temperature of the TD PCM. For example, the PBB/TD/CCD-2 is located at about 32 °C. The isothermal platforms of PBB/TD/CCD composites involve one endothermic and two exothermic processes, which are significantly shorter than those of PBB/TD. The similar pattern has been further proven, as shown in Figure S8. This is attributed to the CCD strengthening the thermal conductivity of TD. A visual proof is that the PBB/TD/CCD basically transforms into a transparent state after

https://doi.org/10.1021/acsomega.4c01570
ACS Omega 2024, 9, 27222−27231

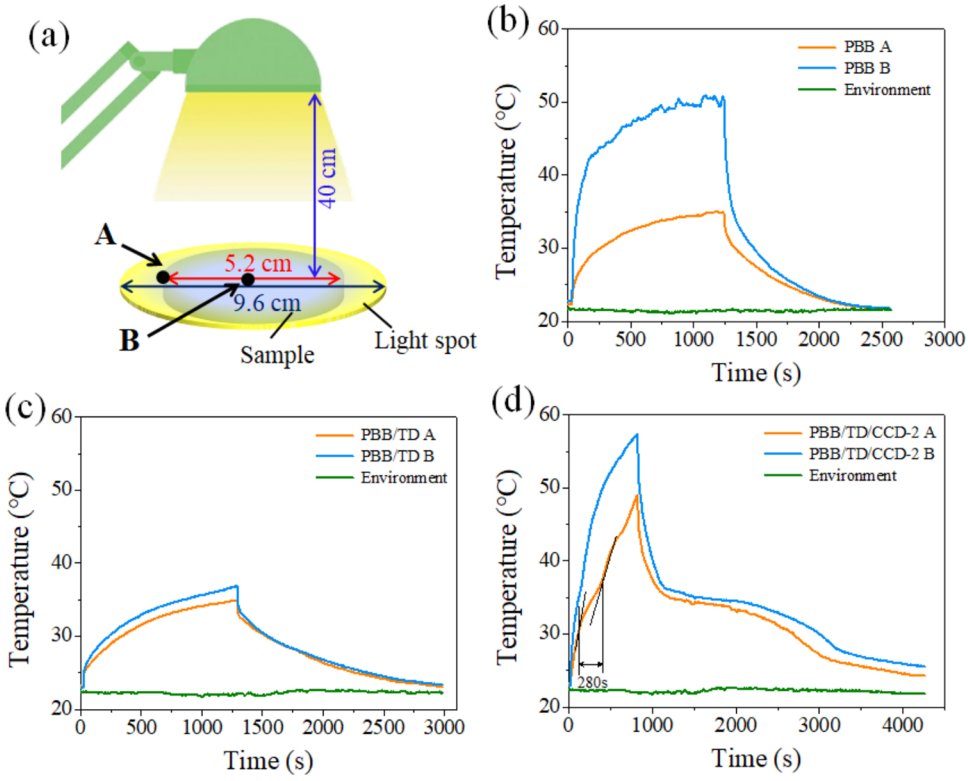

Figure 7. Temperature rise curve of the sample under xenon lamp irradiation. (a) Schematic diagram of the test method. (b) PBB. (c) PBB/TD. (d) PBB/TD/CDD-2.

Table 1. Comparison of the Overall Performance between This Work and Those of Previously Reported Typical PCMs[a]

PCMs	antiliquid leakage	photothermal conversion	ΔH_m [J g^{-1}]	T_{trans} at 25 °C [%]	T_{trans} at 60 °C [%]	refs
wood/PMMA/PEG	yes	no	76.3	63.4	68.1	40
wood/SBO	yes	no	7.2	23.7%	74.9%	41
PGD/DDA	yes	no	41.0	75%	94%	42
PDMS/paraffin	yes	no	na	6%	52%	43
PNIPAm/water	no	no	0	90%	45%	25
wood/CVL/BPA/TD	yes	no	87.9	0	0	44
CFs/PA/OBC	yes	yes	125	0	0	26
EG/MXene/FR/PEG4000	yes	yes	113.3	0	0	27
GA/GCA/HAD/TDA	yes	yes	203.1	0	0	28
PAM/PEG2000	yes	no	39.5	0	0	30
PEG400/PEG2000/NaR	yes	no	109.7	0	0	45
PBB/TD/CCD-2	yes	yes	161.9	0.2%	74.5%	our work

[a]The reported literature cannot simultaneously have a switchable optical transmittance and photothermal conversion due to the opaque nature of the absorbing medium.

being placed at 60 °C for 20 min, as shown in Figure 2a, but about one-third of the PBB/TD composites with the same shape do not melt.

To characterize the photothermal conversion efficiency (η), the temperature−time curve of the PBB/TD/CCD-2 was tested, and the corresponding result is displayed in Figure 7. The photothermal conversion efficiency can be calculated via the following formula:

$$\eta = (m \cdot \Delta H)/(\alpha \cdot \rho \cdot \Delta t)$$

where m is the quality of the PBB/TD/CCD-2 sample, g; ΔH is the latent heat, J g^{-1}; α is the ratio of the composite material to the spot area, %; ρ is the power of xenon lamps, W; and Δt is the melting time of the composite material. Note that this calculation formula is only applicable to the complete melting process of the TD PCM. For the PBB/TD/CCD-2 sample, the corresponding time for the melting process is 280 s. The photothermal conversion efficiency of this composite sample is 74.6%.

Figure S9 shows the TG curves of the PBB, TD, PBB/TD, and PBB/TD/CCD-2 samples. All samples were placed at 25 °C during a relative humidity of 65% for 2 weeks. No weight loss was observed in all samples within the range of 100 °C, indicating that both TD and PBB have no hygroscopicity. The pure TD PCM exhibits a significant weight loss process at 100−200 °C, corresponding to its evaporation process.[39] The PBB polymer enhances the thermal stability of the TD PCM, as the thermal decomposition temperature of PBB exceeds 160 °C. For the PBB/TD and PBB/TD/CCD-2 composites, two obvious weightlessness processes were observed at 120−400

https://doi.org/10.1021/acsomega.4c01570
ACS Omega 2024, 9, 27222−27231

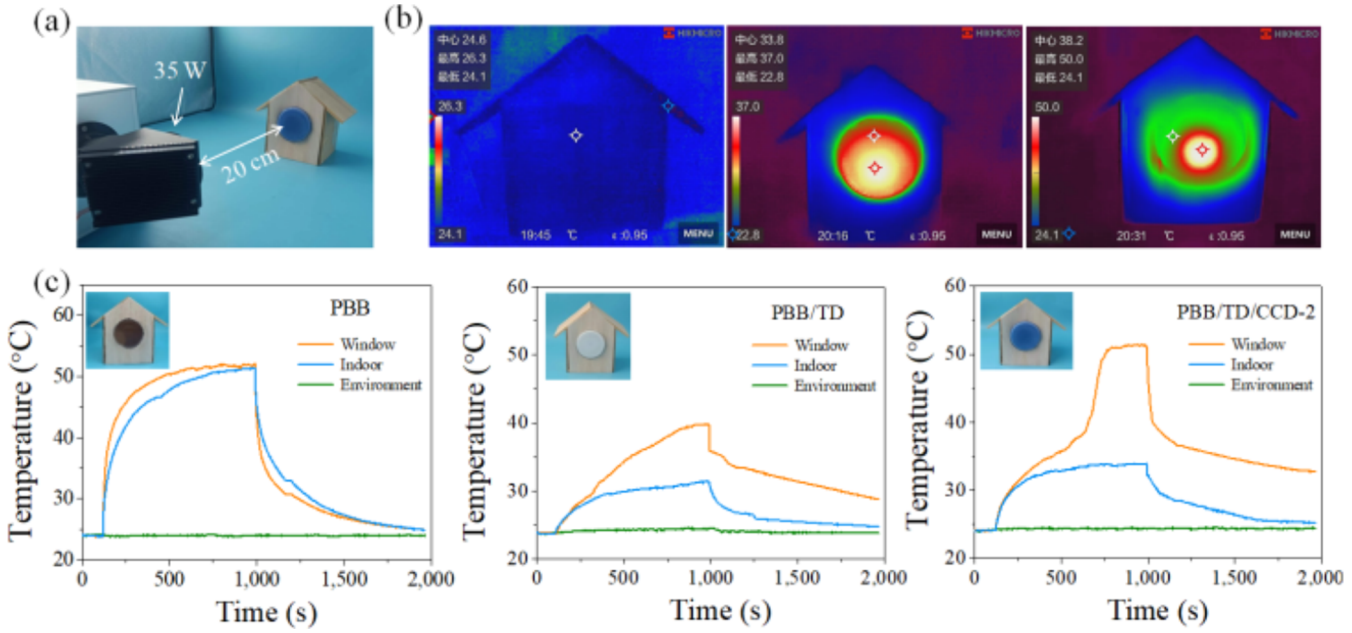

Figure 8. Temperature curves of the thermal-responsive PBB/TD/CCD-2 and the wooden building. (a) Digital photos of the experimental device to test photothermal conversion and storage performance. (b) Thermal imaging photos of the wooden building with the PBB/TD/CCD-2. (c) Temperature−time curves of the wooden building with the PBB, PBB/TD, and PBB/TD/CCD-2 samples.

°C. The former corresponds to the evaporation of the TD PCM, while the latter originates from the thermal decomposition of the PBB polymer network.

2.4. Application in Energy-Saving Buildings. Compared with previously reported PCMs, the thermal-responsive PBB/TD/CCD functional material has antiliquid leakage, switchable optical transparency, photothermal conversion, and thermal energy storage (Table 1). Taking the PBB/TD/CCD-2 composite as an example, it is applied as a passive dimming smart glass in energy-saving buildings (Figure 8). The wooden building was assembled from low-density balsa wood (0.16−0.2 g cm^{-3}) with a thickness of 2 mm to reduce the diffusion rate of heat. Thermal imaging photos confirm the low thermal conductivity of balsa wood (Figure 8b).

The experimental setup is shown in Figure 8a. A xenon lamp is used to provide simulated sunlight, with a power setting of 35 W. The composite PCM is processed into a circular shape that coincides with the light spot. The temperature is measured online by K-type thermocouples, suitable for the environment, energy-saving glass (geometric center of the outer surface), and wooden buildings (geometric center). Figure 8c records the temperature changes of a thermal-responsive window and a wooden building under simulated sunlight irradiation. Note that both heating and cooling times are set to approximately 900 s. Due to the lack of light absorption and avoidance mechanisms, the temperature of the wooden building equipped with the PBB organic glass increases sharply. The wooden building only needs to be irradiated by the xenon lamp for 120 s to reach 40 °C. When solar radiation is stopped, the PBB organic glass and wooden buildings rapidly drop from 51.9 and 51.4 to 30.5 and 33.4 °C, respectively, within 150 s. In the absence of a photothermal conversion medium, the temperature of the PBB/TD PCM increases to 40.0 °C after 900 s of irradiation. During the irradiation period, the PBB/TD PCM has not completely melted, resulting in an increase in the indoor temperature of only 7.3 °C.

The thermally responsive PBB/TD/CCD-2 PCM displays thermal storage/release temperature platforms during the process of turning on/off the xenon lamp. It can reach up to 50 °C after 650 s of irradiation, thanks to the excellent photothermal conversion efficiency of the color changing dye. As a result, the temperature of the wooden building remains above 30 °C for a long time after 130 s of irradiation. After turning off the xenon lamp, it takes 410 s for the indoor temperature to drop to 27.0 °C. For the wooden building equipped with the PBB/TD PCM, it only takes about 120 s to reach the same temperature.

Generally, the utilization rate of solar energy is limited by the solar-to-thermal efficiency and thermal energy storage. The solar-to-thermal efficiency of the PBB/TD/CCD functional material can be increased by introducing a well-matched color changing dye. Thermal energy storage is mainly dependent on the thermal conductivity of the material. The PBB/TD/CCD PCM allows sunlight to penetrate the liquid phase (T_{trans}, 74.5%) and then convert solar energy into thermal energy at the solid−liquid interface of the TD PCM through the well-matched color changing dye. The heat generated by in situ conversion is absorbed by the TD crystal at the phase interface. That is to say, the PBB/TD/CCD PCM eliminates the spatial difference between solar energy conversion and thermal energy storage without considering the thermal conductivity of energy storage materials. Consequently, the as-prepared PBB/TD/CCD PCM has a high photothermal conversion efficiency and thermal storage performance, making it one of the best candidate materials for application in cold regions.

3. CONCLUSIONS

The multifunctional PBB/TD/CCD PCM imitating the polymer hydrogel was developed through a straightforward manufacturing strategy. Luminous transmittance increases from 0.2% at 35 °C to 74.5% at 55 °C, resulting in the as-prepared smart material possessing a thermal-responsive dimming performance. The introduction of a well-matched

https://doi.org/10.1021/acsomega.4c01570
ACS Omega 2024, 9, 27222−27231

color changing dye significantly improves the photothermal conversion efficiency of the PBB/TD/CCD PCM in the low-temperature range but can ignore the negative impact on the transparency of the high-temperature state. The generated heat is then absorbed by the TD PCM. Therefore, photothermal conversion, thermal diffusion, and latent heat storage all occur in the same microzone, providing ideas for the design of energy-saving windows.

4. MATERIALS AND METHODS

4.1. Chemicals and Reagents. All of the experimental chemicals were of analytical grade and used without further purification. *N*-Butyl isobutyrate (BB, 99.0%), ethylene glycol dimethacrylate (EGDMA, 99.0%), azobis(isobutyronitrile) (AIBN, 99.5%), and tetradecanol (99.5%) were supplied by Aladdin (Shanghai, China). The commercial color changing dye comes from Shenzhen Dongfang Color Changing Technology Co., Ltd.

4.2. Preparation of PBB/TD/CCD PCMs. As shown in Figure 1, PBB/TD/CCD PCMs were synthesized by in situ polymerization.[31,32] The TD PCM was heated to 50 °C and then 12 mL of the liquid was added into 8 mL of BB using a pipet. Based on the good compatibility between BB and TD, a transparent mixture was obtained at 50 °C. x g of the CCD (x = 0.05, 0.1, 0.15, and 0.2), 0.016 g of AIBN as an initiator, and 0.052 mL of EGDMA as a cross-linking agent were added in a transparent mixture and stirred continuously at 75 °C for 20 min. Finally, the well-stirred mixture was poured into the customized glass mold and aged in a vacuum drying oven at 65 °C for 24 h to obtain form-stable PCM composites. The as-prepared smart PCMs were referred to as PBB/TD/CCD-x (x = 1−4), and the composition details of the samples are presented in Table 2.

Table 2. Composition Details of the PBB/TD and PBB/TD/CCD Samples

samples	BB (mL)	AIBN (mg)	EGDMA (mL)	TD (mL)	CCD (g)
PBB/TD	8	16	0.052	12	0
PBB/TD/CCD-1	8	16	0.052	12	0.05
PBB/TD/CCD-2	8	16	0.052	12	0.10
PBB/TD/CCD-3	8	16	0.052	12	0.15
PBB/TD/CCD-4	8	16	0.052	12	0.20

4.3. Characterization Techniques. Visible absorption spectra of the temperature-responsive ionic complex liquid were monitored on a PerkinElmer Lambda 950 spectrophotometer to measure the transmittance rate at different temperatures. The transmittance of the plexiglass composite was measured with a commercial tester (LS116, China) at a wavelength of 550 nm. The surface morphology investigation was carried out on a field emission scanning electron microscope (FE-SEM, Hitachi S4800). Before the FE-SEM investigation, the samples were sputtered with gold. Powder X-ray diffraction (XRD) measurements were performed using Cu Kα (λ = 0.154056 nm) radiation with a scan rate of 4° min^{-1} and a step size of 0.03° in the 2θ range of 10 to 60°. FT-IR spectra were recorded on a Fourier transform infrared spectrometer (FT-IR, Nicolet 5700) using a freeze-dried hydrogel pellet (4000−500 cm^{-1}). A differential scanning calorimeter (DSC, TAQ20) was used to investigate the thermal energy storage properties of the prepared form-stable PCM at 5 °C min^{-1} under a constant stream of argon at a flow rate of 50 mL min^{-1}. A Q500 instrument was used for thermogravimetric analysis (TG) with a heating rate of 20 °C min^{-1} from 35 to 800 °C in air. Tensile tests were performed on the hydrogels using a commercial tensile tester (MTS E44) at room temperature with a stretch rate of 100 mm min^{-1}. The test sample was cut into a standard dumbbell-shaped structure with an initial gauge width of 4 mm, a thickness of 2 mm, and a length of 20 mm.

■ ASSOCIATED CONTENT

Supporting Information

The Supporting Information is available free of charge at https://pubs.acs.org/doi/10.1021/acsomega.4c01570.

Experimental details, composition of the commercial CCD, digital photos of the smart glass, visible absorption spectrum, and isothermal endothermic/exothermic curves (PDF)

■ AUTHOR INFORMATION

Corresponding Authors

Haiquan Zhang − *State Key Laboratory of Marine Resource Utilization in South China Sea, Hainan University, Haikou 570228, P. R. China*; orcid.org/0000-0002-8320-6332; Email: haiquanzhang01@hainanu.edu.cn

Ning Wang − *State Key Laboratory of Marine Resource Utilization in South China Sea, Hainan University, Haikou 570228, P. R. China*; Email: wangn02@foxmail.com

Authors

Ling Wang − *State Key Laboratory of Marine Resource Utilization in South China Sea, Hainan University, Haikou 570228, P. R. China*

Fuge Wang − *State Key Laboratory of Marine Resource Utilization in South China Sea, Hainan University, Haikou 570228, P. R. China*

Qiaoming Fang − *State Key Laboratory of Marine Resource Utilization in South China Sea, Hainan University, Haikou 570228, P. R. China*

Songjiao Chen − *State Key Laboratory of Marine Resource Utilization in South China Sea, Hainan University, Haikou 570228, P. R. China*

Wei He − *State Key Laboratory of Marine Resource Utilization in South China Sea, Hainan University, Haikou 570228, P. R. China*

Complete contact information is available at: https://pubs.acs.org/10.1021/acsomega.4c01570

Author Contributions

†H.Q.Z., L.W., and F.G.W. contributed equally to this work. H.Q.Z. conceived the idea and designed the experiments. L.W. and F.G.W. contributed to the material fabrication. L.W., Q.M.F., and W.H. conducted the measurement. S.J.C. and W.H. contributed to the discussion. N.W. analyzed the corresponding results.

Notes

The authors declare no competing financial interest.

■ ACKNOWLEDGMENTS

This work was supported by the National Key Research and Development Program of China (2023YFC2809000), the National Natural Science Foundation of China (Nos.

22327807, U23A20104, and U2167220), the Hainan Province Science and Technology Special Fund (ZDYF2024SHFZ066), the Specific Research Fund of the Innovation Platform for Academicians of Hainan Province (YSPTZX202214 and YSPTZX202316), and the Innovation Fund for Scientific and Technological Personnel of Hainan Province (KJRC2023B01).

■ ABBREVIATIONS

HVAC, heating, ventilation, and air-conditioning; PCM, phase change material; PNIPAm, poly(*N*-isopropylacrylamide); PPCs, porous polymer coatings; PBB, poly(*n*-butyl isobutyrate); TD, tetradecanol; CCD, color changing dye; BB, *n*-butyl isobutyrate; AIBN, azobis(isobutyronitrile); EGDMA, ethylene glycol dimethacrylate

■ REFERENCES

(1) Qian, Y.; Chai, C.; Qi, P.; et al. Integrated thermoelectric design inspired by ionic liquid microemulsion-based gel with regulatable dual-temperature responsiveness. *ACS Appl. Polym. Mater.* **2023**, *5*, 2983−2994.
(2) Shi, H.; Chen, Q. Building energy management decision-making in the real world: A comparative study of HVAC cooling strategies. *J. Build. Eng.* **2021**, *33*, No. 101869.
(3) Yu, X.; Ergan, S.; Dedemen, G. A data-driven approach to extract operational signatures of HVAC systems and analyze impact on electricity consumption. *Appl. Energy* **2019**, *253*, No. 113497.
(4) Ding, Y.; Wei, M.; Liu, R. Channel parameters for the temperature distribution of a battery thermal management system with liquid cooling. *Appl. Therm. Eng.* **2021**, *186*, No. 116494.
(5) Tasri, A.; Susilawati, A. Effect of cooling water temperature and space between cooling pipes of post-cooling system on temperature and thermal stress in mass concrete. *J. Build. Eng.* **2019**, *24*, No. 100731.
(6) Llordés, A.; Garcia, G.; Gazquez, J.; Milliron, D. J. Tunable near-infrared and visible-light transmittance in nanocrystal-in-glass composites. *Nature* **2013**, *500*, 323−326.
(7) Gao, Y.; Wang, S.; Kang, L.; et al. VO_2Sb:SnO_2 composite thermochromic smart glass foil. *Energy Environ. Sci.* **2012**, *5*, 8234−8237.
(8) Hee, W. J.; Alghoul, M. A.; Bakhtyar, B.; et al. The role of window glazing on daylighting and energy saving in buildings. *Renewable Sustainable Energy Rev.* **2015**, *42*, 323−343.
(9) Kalnæs, S. E.; Jelle, B. P. Phase change materials and products for building applications: a state-of-the-art review and future research opportunities. *Energy Build.* **2015**, *94*, 150−176.
(10) Lv, X.; Shao, M.; Zhu, X.; et al. Thermally cross-linked copolymer for highly transparent to multicolor-showing electrochromic materials. *ACS Appl. Polym. Mater.* **2023**, *5*, 3595−3603.
(11) Zheng, R.-r.; Huang, T.; Niu, H.; et al. Multifunctional flexible polyimides for electroactive devices with electrochromic, electrofluorochromic, and photodetection properties. *ACS Appl. Polym. Mater.* **2021**, *3*, 1338−1348.
(12) Liu, Y.; Lu, C.; Bian, S.; et al. Reversible photo-responsive smart wood with resistant to extreme weather. *J. Mater. Sci.* **2022**, *57*, 3337−3347.
(13) Kwon, H.; Lee, K.; Hur, K.; et al. Optically switchable smart windows with integrated photovoltaic devices. *Adv. Energy Mater.* **2015**, *5*, No. 1401347.
(14) Ding, Y.; Duan, Y.; Yang, F.; et al. High-transmittance pNIPAm gel smart windows with lower response temperature and stronger solar regulation. *Chem. Eng. J.* **2022**, *460*, No. 141572.
(15) Zhou, Y.; Cai, Y.; Hu, X.; Long, Y. Temperature-responsive hydrogel with ultra-large solar modulation and high luminous transmission for "smart window" applications. *J. Mater. Chem. A* **2014**, *2*, 13550−13555.
(16) Louloudakis, D.; Vernardou, D.; Spanakis, E.; et al. Atmospheric pressure chemical vapor deposition of amorphous tungsten doped vanadium dioxide for smart window applications. *Adv. Mater. Lett.* **2016**, *7*, 192−196.
(17) Tao, X.; Yang, A.; Yang, S.; et al. Leading components and pressure-induced color changes in N-doped lutetium hydride. *Sci. Bull.* **2023**, *68*, 1372−1378.
(18) Zhou, Y.; Dong, X.; Mi, Y.; et al. Hydrogel smart windows. *J. Mater. Chem. A* **2020**, *8*, 10007−10025.
(19) Zhang, H.; Liu, J.; Shi, F.; et al. A novel bidirectional fast self-responsive PVA-PNIPAM/LimCsnWO_3 composite hydrogel for smart window applications. *Chem. Eng. J.* **2022**, *431*, No. 133353.
(20) Huang, Z.; Chen, S.; Lv, C.; et al. Infrared characteristics of VO_2 thin films for smart window and laser protection applications. *Appl. Phys. Lett.* **2012**, *101*, No. 191905.
(21) Zhao, Z.; Liu, Y.; Wang, D.; et al. Sn dopants improve the visible transmittance of VO_2 films achieving excellent thermochromic performance for smart window. *Sol. Energy Mater. Sol. Cells* **2020**, *209*, No. 110443.
(22) Qiu, Z.; Wang, S.; Wang, Y.; et al. Transparent wood with thermo-reversible optical properties based on phase-change material. *Compos. Sci. Technol.* **2020**, *200*, No. 108407.
(23) Zhang, H.; Mai, J.; Li, S.; et al. Multi-functional phase change materials with anti-liquid leakage, shape memory, switchable optical transparency and thermal energy storage. *Adv. Compos. Hybrid Mater.* **2022**, *5*, 2042−2050.
(24) Zhou, Y.; Wang, S.; Peng, J.; et al. Liquid thermo-responsive smart window derived from hydrogel. *Joule* **2020**, *4*, 2458−2474.
(25) Mandal, J.; Jia, M.; Overvig, A.; et al. Porous polymers with switchable optical transmittance for optical and thermal regulation. *Joule* **2019**, *3*, 3088−3099.
(26) Zhang, P.; Wang, Y.; Qiu, Y.; et al. Novel composite phase change materials supported by oriented carbonfibers for solar thermal energy conversion and storage. *Appl. Energy* **2024**, *358*, No. 122546.
(27) Wang, Y.; Zhao, L.; Zhan, W.; et al. Flame retardant composite phase change materials with MXene for lithium-ion battery thermal management systems. *J. Energy Storage* **2024**, *86*, No. 111293.
(28) Wang, C.; Wang, L.; Liang, W.; et al. Enhanced light-to-thermal conversion performance of all-carbon aerogels based form-stable phase change material composites. *J. Colloid Interface Sci.* **2022**, *605*, 60−70.
(29) Zhao, T.; Zhang, T.; Xu, Z.; Zhao, Y. Emulsion-based, flexible and recyclable aerogel composites for latent heat storage. *J. Colloid Interface Sci.* **2022**, *627*, 72−80.
(30) Zhang, H.; Liu, Z.; Mai, J.; et al. Super-elastic smart phase change material (SPCM) for thermal energy storage. *Chem. Eng. J.* **2021**, *411*, No. 128482.
(31) Wan, S.; Zhou, S.; Huang, X.; et al. Effect of aromatic petroleum resin on damping properties of polybutyl methacrylate. *Polymer* **2020**, *12*, No. 543.
(32) Hexemer, A.; Müller-Buschbaum, P. Advanced grazing-incidence techniques for modern soft-matter materials analysis. *IUCrJ* **2015**, *2*, 106−125.
(33) Kreuzer, L. P.; Widmann, T.; Bießmann, L.; et al. Phase transition kinetics of doubly thermoresponsive poly(sulfobetaine)-based diblock copolymer thin films. *Macromolecules* **2020**, *53*, 2841−2855.
(34) Brett, C. J.; Mittal, N.; Ohm, W.; et al. Water-induced structural rearrangements on the nanoscale in ultrathin nanocellulose films. *Macromolecules* **2019**, *52*, 4721−4728.
(35) Alkan, C.; Alakara, E. H.; Aksoy, S. A.; Demir, İ. Cement mortar composites including 1-tetradecanol@PMMA Pickering emulsion particles for thermal energy management of buildings. *Chem. Eng. J.* **2023**, *476*, No. 146843.
(36) Chi, B.; Yao, Y.; Cui, S.; Jin, X. Preparation of graphene oxide coated tetradecanol/expanded graphite composite phase change material for thermal energy storage. *Mater. Lett.* **2021**, *282*, No. 128666.
(37) Liu, C.; Wang, L.; Li, Y.; et al. Fe_3O_4/carbon-decorated graphene boosts photothermal conversion and storage of phase change materials. *J. Colloid Interface Sci.* **2024**, *657*, 590−597.

https://doi.org/10.1021/acsomega.4c01570
ACS Omega 2024, 9, 27222−27231

(38) Cao, X.; Yang, L.; Yan, L.; et al. ZnO nanorods loading with fatty amine as composite PCMs device forefficient light-to-thermal and electro-to-thermal conversion. *J. Colloid Interface Sci.* **2023**, *629*, 307−315.
(39) Geng, X.; Li, W.; Wang, Y.; et al. Reversible thermochromic microencapsulated phase change materials for thermal energy storage application in thermal protective clothing. *Appl. Energy* **2018**, *217*, 281−294.
(40) Montanari, C.; Li, Y.; Chen, H.; et al. Transparent wood for thermal energy storage and reversible optical transmittance. *ACS Appl. Mater. Interfaces* **2019**, *11*, 20465−20472.
(41) Qiu, Z.; Wang, S.; Wang, Y.; et al. Transparent wood with thermo-reversible optical properties based on phase change material. *Compos. Sci. Technol.* **2020**, *200*, No. 108407.
(42) Zhang, C.; Deng, H.; Kenderes, S. M.; et al. Chemically interconnected thermotropic polymers for transparency-tunable and impact-resistant windows. *ACS Appl. Mater. Interfaces* **2019**, *11*, 5393−5400.
(43) Owuor, P. S.; Chaudhary, V.; Woellner, C. F.; et al. High stiffness polymer composite with tunable transparency. *Mater. Today* **2018**, *21*, 475−482.
(44) Yang, H.; Wang, Y.; Yu, Q.; et al. Composite phase change materials with good reversible thermochromic ability in delignified wood substrate for thermal energy storage. *Appl. Energy* **2018**, *212*, 455−464.
(45) Sun, Q.; Zhang, H.; Xue, J.; et al. Flexible phase change materials for thermal storage and temperature control. *Chem. Eng. J.* **2018**, *353*, 920−929.

https://doi.org/10.1021/acsomega.4c01570
ACS Omega 2024, 9, 27222−27231